#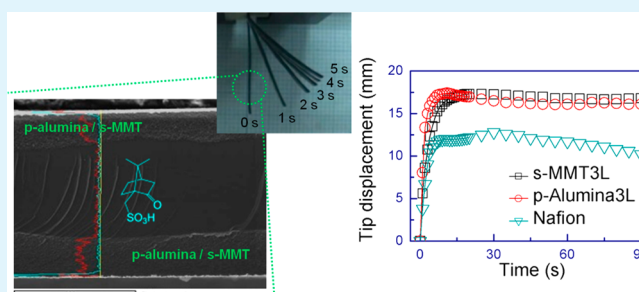 Ionic Polymer−Metal Composite Actuators Based on Triple-Layered Polyelectrolytes Composed of Individually Functionalized Layers

Jang-Woo Lee,[†,§] Young-Tai Yoo,*,[†] and Jae Yeol Lee[‡]

[†]Department of Materials Chemistry and Engineering, College of Engineering, Konkuk University, 1 Hwayang-dong, Gwangjin-gu, Seoul 143-701, Republic of Korea

[‡]Composite Group, Agency for Defense Development, Yuseong P. O. Box 35-44, Daejeon 305-600, Republic of Korea

S *Supporting Information*

ABSTRACT: Ionic polymer−metal composite (IPMC) actuators based on two types of triple-layered Nafion composite membranes were prepared via consecutive solution recasting and electroless plating methods. The triple-layered membranes are composed of a Nafion layer containing an amphiphilic organic molecule (10-camphorsulfonic acid; CSA) in the middle section (for fast and large ion conduction) and two Nafion/modified inorganic composite layers in the outer sections (for large accumulation/retention of mobile ions). For construction of the two types of IPMCs, sulfonated montmorillonite (MMT) and polypyrrole (PPy)-coated alumina fillers were incorporated into the outer layers. Both the triple-layered IPMCs exhibited 42% higher tip displacements at the maximum deflections with a negligible back-relaxation, 50−74% higher blocking forces, and more rapid responses under 3 V dc, compared with conventional single-layered Nafion-IPMCs. Improvements in cyclic displacement under a rectangular voltage input of 3 V at 1 Hz were also made in the triple-layered configurations. Compared with single-layered IPMCs consisting of the identical compositions with the respective outer composite layers, the bending rates and energy efficiencies of both the triple-layered IPMCs were significantly higher, although the blocking forces were a bit lower. These remarkable improvements were attributed to higher capacitances and Young's moduli as well as a more efficient transport of mobile ions and water through the middle layer (Nafion/CSA) and a larger accumulation/retention of the mobile species in the outer functionalized inorganic composite layers. Especially, the triple-layered IPMC with the PPy-modified alumina registered the best actuation performance among all the samples, including a viable actuation even at a low voltage of 1.5 V due to involving efficient redox reactions of PPy with the aid of hygroscopic alumina.

KEYWORDS: *ionic polymer−metal composites (IPMCs), actuator, alumina, polypyrrole, montmorillonite, amphiphilic organic molecule, Nafion*

■ INTRODUCTION

Among electroactive polymers (EAPs) such as conductive polymers, dielectric elastomers, ionic polymer−metal composites (IPMCs), ionic polymer gels, carbon nanotubes, and electroactive papers, the IPMC is an attracting actuator due to its large and fast bending deformation produced by a fairly low external electrical stimulus of 1−5 V.[1,2] Conversely, the IPMC also offers a mechanoelectrical response (i.e., sensing capability). Due to these fascinating features, intense studies in the IPMC field have been recently reported.[3−7] The IPMC is typically composed of an ion-conductive layer and two platinum electrode layers, and bends through the cathode-directional transport of mobile cations and water in the interior when electric potentials are applied between the two metallic electrodes.[2]

Using Nafion® as the ion-conductive matrix of an IPMC would require improvements in its stiffness, ion conductivity, and the back-diffusion of excess charges induced by small pK_a (approximately −6) in the IPMC device.[5] The stiffness, ion conductivity, and back-diffusion are deeply related to the actuation force, response rate, and back-relaxation of IPMC actuator, respectively. The back-relaxation phenomenon is one of the major drawbacks of IPMCs, in which the IPMC strip cannot hold the strain after reaching a maximum forward displacement under an applied dc potential. This limits the motion control and operational frequency range.[8,9] A rapid desorption of water out of the Nafion is also one of the drawbacks, which accelerates the performance decay as well as the back-relaxation behavior.[10,11]

These drawbacks can readily be improved via surface and internal modifications of the commercial ionomer.[12−15] Chao et al. added hygroscopic γ-alumina particles to the interface between the Nafion layer and the anode catalyst layer in preparing proton exchange membrane fuel cells (PEMFCs).

This rendered high performances at low-humidity conditions to the fuel cell.[12] Huang et al. electrochemically modified the Nafion membrane with polyaniline, one of the inherently conductive polymers. The direct methanol fuel cells (DMFCs) with the modified Nafion membranes displayed significantly decreased methanol permeabilities up to 10 times lower than that with the pristine Nafion at the sacrifice of proton conductivity.[13] In the IPMC application, Nam and Lee et al. introduced Nafion/montmorillonite (MMT) and Nafion/multi-walled carbon nanotube (MWNT) composite membranes into the IPMC structure, and their IPMCs generated stronger actuation forces than the pristine Nafion-based one.[14,15] The reinforced performances were related to the improvement in mechanical modulus and electrochemical property. Recently, the modification of electrodes with highly porous materials is being advanced for the purpose of enhancing capacitances of electric double layers formed along the interface of electrode/electrolyte in ionic EAPs.[16] It was reported that higher capacitances in the ionic EAPs usually lead to larger deformations under applied potentials.[17]

In recent studies, a sulfonic acid-functionalized MMT was incorporated into nanostructured styrenic block copolymer ionomers (SSPB) to prepare the nanocomposite membranes as the polyelectrolyte layer of IPMC.[5,6,18] Additional ionic sites rendered by the sulfonation on the interlayer space of the layered MMT as well as its external surface gave strong interactions among the sulfonic groups on the MMT, the mobile ions, and sulfonic groups in the SSPB matrix, which resulted in a well-dispersed intercalation morphology of the nanocomposite polyelectrolyte; thus, this modification improved the mechanical property and the ion-transporting behavior. The sulfonic acid-functionalized MMT-incorporated IPMC revealed a largely enhanced bending displacement, rate, and force with a very limited back-relaxation behavior. We also reported that the addition of a PPy/alumina composite filler into the Nafion polyelectrolyte layer of IPMC greatly contributed to the actuation performance due to the electro-chemical redox reactions of PPy in an abundantly humidified regime by the neighboring hygroscopic alumina moieties.[19] With the largely enhanced performance, the Nafion/PPy/alumina system showed the low-voltage-operable character and the negligible back-relaxation as well. In our ongoing work, it was observed that the incorporation of an amphiphilic organic molecule (10-camphorsulfonic acid; CSA) into Nafion greatly enhanced the ionic conductivity (up to 45% at a CSA content of 8 wt %) due to the high concentration and narrow size distribution of ionic clusters in the CSA-incorporated Nafion matrix. The possibility that the CSA molecules would leak out of the polymer matrix was excluded from a long-term leak test.

From the precedent research mentioned above, we devised IPMCs based on triple-layered membranes composed of a Nafion layer containing CSA in the middle section (for fast and large ion conduction) and two Nafion/modified inorganic composite layers in the outer sections (for large accumulation/retention of mobile ions). As the fillers for the outer composite layers, the sulfonic-acid-functionalized MMT and the PPy-functionalized alumina are engaged. Both configurations for the polyelectrolyte layer of IPMC promote the bending rate and displacement and minimize the back-relaxation phenomenon. The bending performances of IPMCs based on the two proposed triple-layered membranes are compared with each other and those of the respective single-layered composite membranes consisting of the identical composition with each outer composite layer, through electromechanical measurements.

■ EXPERIMENTAL SECTION

Materials. A 20 wt % Nafion dispersion (DE-2021, DuPont), with a total acid capacity of 0.95 meq g^{-1} (0.95 mmol H$^+$ per 1 g polymer), was engaged in fabricating a polyelectrolyte film of IPMC. Pyrrole (purity: 98%), hydrated ferric sulfate (Fe$_2$(SO$_4$)$_3$·xH$_2$O, purity: 97%), and sodium dodecyl sulfate (SDS, purity: 99+%) were purchased from Aldrich, and α-alumina (ALO14PB, particle size: 1 μm) was purchased from Kojundo Chemical Laboratory Co., Ltd., in Japan. The MMT (Cloisite Na$^+$), which is a natural MMT with a cation exchange capacity of 0.926 meq/1 g clay, was obtained from Southern Clay Products. Both 3-mercaptopropyl-trimethoxy silane (3-MPTMS) and 10-camphorsulfonic acid (CSA) were purchased from Aldrich. The chemical structure of CSA is shown in Figure S1 of Supporting Information.

Preparation of Functionalized Inorganic Fillers. According to a procedure in the literature,[5] the functionalization of MMT was performed via condensation with 3-MPTMS and the following oxidation to obtain the sulfonated MMT, which endows them with additional ion-hopping sites and better dispersion in the polyelectrolyte matrices. The sulfonic group density of the functionalized MMT was 0.33 mmol g^{-1} (mmol of grafted sulfonic acid groups per g of MMT), evaluated from thermogravimetry. Meantime, the functionalization of α-alumina was performed via in-situ chemical polymerization of pyrrole on the surface of alumina as described in our previous work,[19] and thus the PPy-coated alumina particles (PPy:alumina = 1:1.65, w/w) were obtained. The modified MMT and alumina are hereafter denoted as "s-MMT" and "p-alumina", respectively. The graphic procedures for the preparation of s-MMT and p-alumina are provided in Figures S2 and S3 of Supporting Information, respectively.

Preparation of Triple-Layered Membranes and IPMCs. The triple-layered membranes were prepared by a consecutive solution recasting technique, which is an easy and useful tool for the construction of layer-by-layer configurations (A schematic representation showing the consecutive solution recasting method is exhibited in Figure S4 of Supporting Information.).[20] The triple-layered membranes in this study were composed of one Nafion layer containing CSA (8 wt %) in the middle section and two Nafion layers containing the functionalized s-MMT (4 wt %) or p-alumina (7.95 wt %) in the outer sections. A Nafion/filler solution for one outer layer was first cast into a glass mold, and a Nafion/CSA solution for the middle layer and the first Nafion/filler solution for the other outer layer after appropriate drying of each layer were cast onto the precast surfaces in turn. The temperature in the drying steps for forming each layer was 60 °C, and each drying step was terminated through casting the next solution at a point at which the fluidity of the precast solution remained to a limited extent. The remained fluidity of the precast solution could afford chain entanglement between the precast solution and the next solution, leading to a seamless interface between the unit layers of the resulting triple-layered membrane, thereby enabling continuous transport of mobile ions between the layers. Prior to cast, all the solutions were thoroughly stirred and ultrasonicated for 30 min at a power of 30 W. Finally, the obtained membranes were annealed at 130°C for 2 h to develop the morphology, which gave the Nafion membranes desirable ionic conductivities and mechanical properties, and

insolubility in most solvents.[21,22] For rational comparison, the thickness of the middle and outer layers could be controlled by varying the amount of each cast solution and measured 240 ± 15 and 100 ± 15 μm, respectively. Normal single-layered membranes as base samples were obtained via a typical one-step solution casting method. The total thicknesses of the conventional single-layered and multilayered membranes in the hydrated states were in a narrow range of 0.32−0.45 mm. Configurations and some physical properties of the membranes are summarized in Table 1. IPMCs were fabricated via chemical plating of platinum on both membrane surfaces as detailed elsewhere.[5] For better actuation performance, the Li$^+$-form IPMCs were obtained by immersion in a 1 N aqueous lithium hydroxide solution for at least 12 h.

Characterization. A scanning electron microscope (SEM, JSM-6380, Jeol)-combined energy-dispersive X-ray spectrometer (EDS, INCA X-Act, Oxford Instruments) was used to observe the cross-sectional view of IPMCs based on the triple-layered polyelectrolytes. Proton conductivity (σ) was measured underwater using an electrochemical impedance analyzer (IM6ex, Zahner) and a custom-made cell for the normal four-probe technique at room temperature. A universal test machine (Model 4465, Instron) was used to assess the Young's modulus (E) of membranes. For actuation experiments, IPMC strips with dimensions of 25 mm in length and 5 mm in width were vertically fixed to 5 mm length by a gold grip, and thus the actual free length of the strips was 20 mm. The actuation test was performed at ambient conditions (temp: 25±2 °C; relative humidity: 25±3%) immediately after an IPMC strip stored in a vessel filled with deionized water was taken up and then promptly wiped with a filter paper to remove water on the surface of the IPMC strip. Electric power was applied using an AC source/analyzer (Model 6811B, Agilent). The real-time bending displacement (δ) was measured using a laser sensor (LB-11, Keyence) and a CCD camera connected to a computer by a data acquisition (DAQ) system (SCB-68, National Instruments). The blocking force (F) was taken with a load cell (CB1-G150, Dacell) when the force generated at the tip of IPMC strip reached the steady state. A multichannel potentiostat/galvanostat (WMPG1000, Wonatech) was used to evaluate the electrochemical characteristics of IPMC.

■ RESULTS AND DISCUSSION

The cross-sectional SEM image and EDS spectra of an IPMC actuator based on a triple-layered composite membrane (s-MMT3L) are shown in Figure 1. From the two EDS profiles assigned to silicon (red line) and platinum (cyan line), the s-MMT containing silicon was identified in the two outer layers of the polyelectrolyte, and the thickness of the platinum electrode was approximately 10 μm. It was also observed from the SEM image that the dispersity of s-MMT in the outer layers was very high, and the Nafion/s-MMT nanocomposite layer had an intercalation morphology, evidenced from X-ray diffraction (Figure S5 of Supporting Information). A high dispersity of p-alumina in the Nafion matrix was also confirmed through SEM observation (Figure S6 of Supporting Information). As can be seen in Table 1, this triple-layered configuration gave mechanical gains (s-MMT3L: 11.3 %; p-Alumina3L: 6.1%) and ion-conductive gains to some extent to the membranes, which promisingly enhance the bending actuation performance of IPMC. Also, as shown in Table 2, the triple-layered membranes intervened between both platinum electrodes; that is, the IPMCs based on the triple-
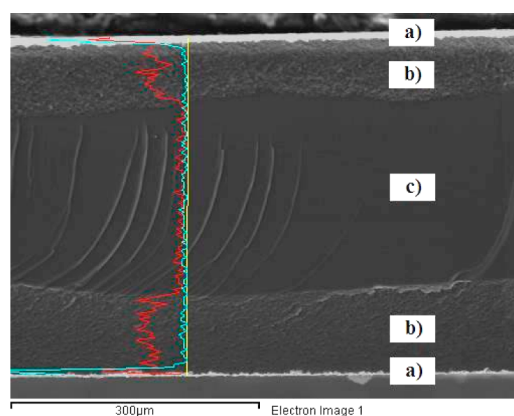

Figure 1. Scanning electron micrograph and energy-dispersive X-ray spectra of a cross section of the IPMC actuator based on triple-layered composite membranes. Designations (a), (b), and (c) represent the platinum electrode, the outer electrolyte layer (Nafion/modified filler), and the middle electrolyte layer (Nafion/CSA), respectively.

layered membranes possessed higher capacitances (C) than those of the IPMCs with pristine Nafion and Nafion/CSA membranes, while being comparable to each single-layered counterpart. Furthermore, the seamless interface between the middle and outer electrolyte layers is an evidence of strong adhesion, thereby persisting continuous transport of mobile ions between the layers, which is indispensable for fast ionic response in the IPMC system and many other ionic devices as well.

Time-dependent bending displacements of the triple-layered IPMCs recorded at the tip of IPMC cantilevers are shown and compared with single-layered IPMCs (Nafion/CSA- and Nafion-IPMCs) in Figure 2. Both the triple-layered IPMCs with higher capacitances exhibited significantly higher tip displacements at the maximum deflection compared with those of the single-layered IPMCs. The values for s-MMT3L, p-Alumina3L, Nafion/CSA, and Nafion samples were 17.3, 17.4, 14.2, and 12.2 mm, respectively, which values were listed in Table 2. Bending response within the initial 5 s was also assessed. It was observed that the addition of CSA into the Nafion matrix improved the initial bending rate of IPMC. In the case of p-Alumina3L-IPMC, the initial rate in 1 s was nearly identical with that of the Nafion/CSA-IPMC. However, the bending response of the s-MMT3L-IPMC was slower than that of the p-Alumina3L-IPMC, probably due to the tortuous ionic path caused by intercalated MMT platelets in the Nafion matrix.[23,24] The increase in displacement was sustained for a few seconds in both the triple-layered IPMCs and the displacements were saturated with much larger values within a narrow time scale of 20 s. The blocking force at the tip of IPMC strip was also measured under 3 V dc, and the values are listed in Table 2. The blocking forces of the s-MMT3L- and p-Alumina3L-IPMCs were 1.7 and 1.5 times higher than that of Nafion-IPMC (0.42 g$_f$). It could be attributed to be the result of the higher maximum displacements and moduli of the triple-layered IPMCs since the blocking force depends on both the displacement and the stiffness.[25] Besides, the back-relaxation behavior was observed to a very limited extent in both the triple-layered IPMCs during the test period. It was expected that the hygroscopic nature of s-MMT and p-alumina fillers and additionally the tortuous ionic path formed by dispersed MMT platelets in the outer layer strongly retained water and mobile ions once it moved into the outer layer,[5,19,23,24] thus

**Table 1. Composition, Water Uptake, Proton Conductivity, and Young's Modulus of Triple-Layered Membranes**

no. of layer	configuration	code	WU^a (wt %)	σ (S cm^{-1})	E^b (MPa)	$t_d{}^c$ (mm)	$t_h{}^d$ (mm)
3	Naf(4% s-MMT)/Naf(8% CSA)/Naf(4% s-MMT)	s-MMT3L	24.2	0.090	392	0.40	0.44
	Naf(7.95% p-alumina)/Naf(8% CSA)/Naf(7.95% p-alumina)	p-Alumina3L	23.6	0.085	326	0.36	0.40
1	Naf/(4% s-MMT)	s-MMT1L	24.5	0.088	442	0.38	0.42
	Naf/(7.95% p-alumina)	p-Alumina1L	24.0	0.080	347	0.40	0.45
	Naf/8% CSA	Nafion/CSA	23.3	0.123	226	0.26	0.32
	pristine Nafion	Nafion	22.3	0.085	232	0.30	0.34

^{a}Water uptake: to determine the water content of each membrane, the membrane was fully dried in a vacuum for 12 h and weighed. After that, the membrane fully swollen in deionized water for 24 h at room temperature was wiped with a filter paper and then reweighed immediately. The water uptake was obtained from the following formula: water uptake (wt %) = ((weight of wet sample − weight of dry sample)/weight of dry sample) × 100. ^{b}Young's modulus measured in the dry state. ^{c}Thickness in the dry state. ^{d}Thickness in the hydrated state.

Table 2. Summary of Electromechanical Characteristics of IPMCs Based on Triple-Layered Membranes

membrane	C (F cm^{-2})	max δ^a (mm)	F^b (g$_f$)	$Q_d{}^c$ (mC cm^{-2})	δ^c (mm)	$\delta_c{}^c$ (mm/(mC cm^{-2}))
s-MMT3L	5.90	17.3	0.73	766.4	13.5	0.018
p-Alumina3L	4.53	17.4	0.63	629.8	16.5	0.026
s-MMT1L	3.37	17.2	0.94	732.3	8.2	0.011
p-Alumina1L	6.84	17.5	0.82	849.7	13.8	0.016
Nafion/CSA	2.86	14.2	0.34	752.2	13.6	0.018
Nafion	2.22	12.2	0.42	537.1	11.0	0.020

^{a}Maximum tip displacement obtained under 3 V dc. ^{b}Blocking force taken at the steady state under 3 V dc. ^{c}Tip displacement (δ) and charge-specific displacement (δ_c) obtained for initial 5 s under 3 V dc.
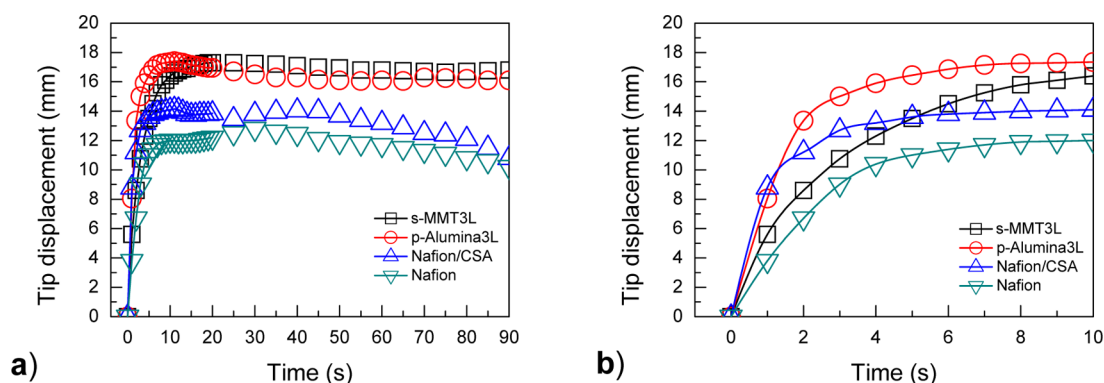
Figure 2. Time-dependent tip displacement of IPMC actuators based on triple-layered composite membranes recorded for 90 s under an applied potential of 3 V dc. (b) Magnification of (a) with a shorter time scale (0−10 s).
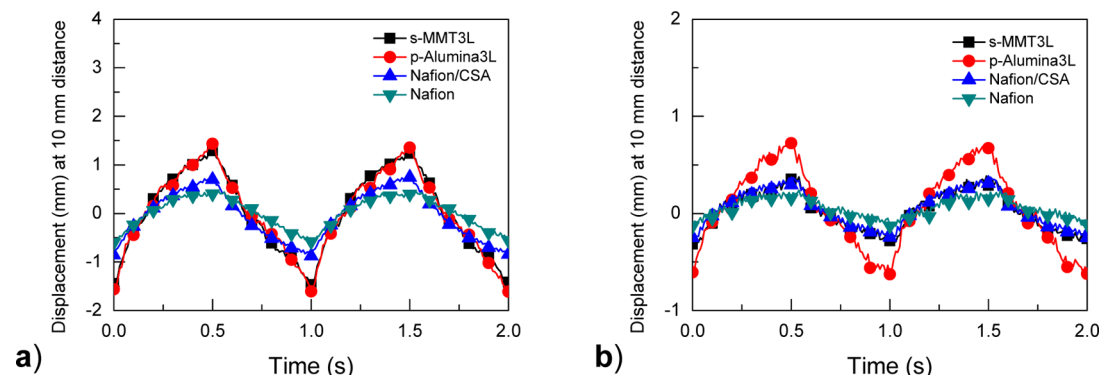
Figure 3. Cyclic displacement of IPMC actuators based on triple-layered composite membranes recorded under rectangular voltage pulses of (a) 3 V and (b) 1.5 V at a frequency of 1 Hz. The displacement was measured at 10 mm distance from the gold grip and the maximum peak-to-peak value was taken within an operation period of 0−40 s.

decelerating the back-relaxation rate under the applied dc potential.

Cyclic horizontal displacement under 3 V and 1.5 V rectangular voltage inputs of 1 Hz was also evaluated at 10 mm distance from the grip and the maximum peak-to-peak value was taken within an operation period of 0−40 s (Figure 3). At 3 V, both cyclic displacements of the triple-layered IPMCs surpassed those of the single-layered IPMCs, although
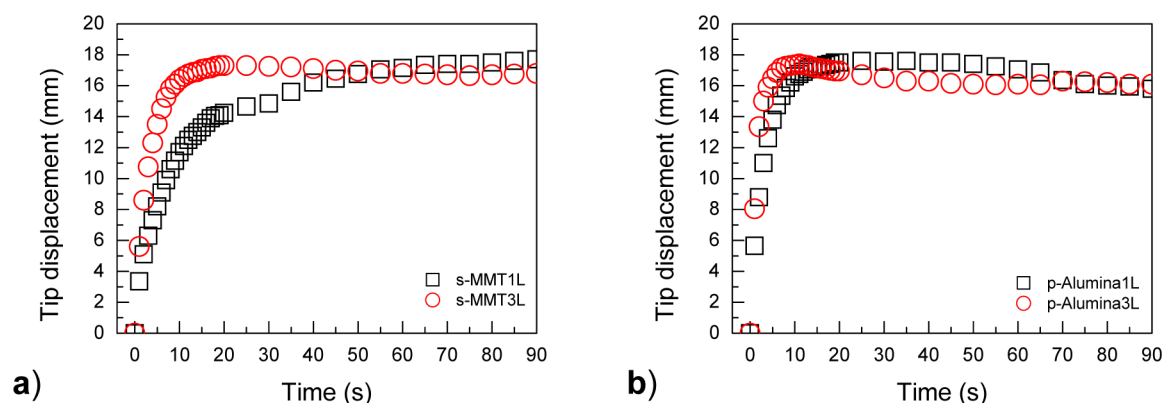
Figure 4. Comparative actuation performance of triple- and single-layered IPMCs under an applied potential of 3 V dc: (a) s-MMT and (b) p-alumina.

the dc bending response of the s-MMT3L-IPMC was slower than that of the p-Alumina3L- and Nafion/CSA-IPMCs. The unexpectedly fast cyclic response of the s-MMT3L-IPMC was due to the largest increase in displacement during the operation period of 0−40 s, although the initial peak-to-peak value was smaller than that of the Nafion/CSA-IPMC. This might be related to effective channeling of ionic paths or optimizing of water content[26] during the fast alternate actuation. In 2009, we reported that the Nafion/PPy/alumina system produces quite a large bending motion even under a low electric potential of 1.5 V due to the effective redox reactions of PPy by the neighboring hygroscopic alumina moieties.[19] The outstanding low-voltage-operable character, in this study, was also observed in the p-Alumina3L-IPMC. The peak-to-peak values of the p-Alumina3L-IPMC under a rectangular voltage input of 1.5 V at 1 Hz exceeded at least 2 times compared with that from the other IPMCs. Consequently, the validity of the outer inorganic composite layers in both the triple-layered IPMCs for the contribution to the actuation performance was demonstrated.

To validate the middle layer (Nafion/CSA) in the triple-layered architecture, the s-MMT3L- and p-Alumina3L-IPMCs were compared with the respective single-layered counterparts (i.e., s-MMT1L- and p-Alumina1L-IPMCs) in terms of bending rate, maximum displacement, and blocking force. As shown in Figure 4, the insertion of the middle layer with the fast ion-transporting ability into the s-MMT1L and p-Alumina1L membranes greatly enhanced the bending rates of the IPMCs, especially in the case of the s-MMT type. However, the maximum displacements were almost identical for the triple-layered IPMCs and the single-layered counterparts. This roughly matched the capacitance results of Table 2, although some fluctuating tendency was observed. The capacitance-dependent displacements of IPMCs observed in this study support the experimental results which Akle and Leo et al. reported previously.[17] On the other hand, it was evaluated that the blocking forces of the triple-layered IPMCs were smaller than those of the single-layered counterparts, as shown in Table 2, which shows a trade-off between displacement and force in terms of the mechanical modulus of the strip.

Finally, we evaluated the charge-specific displacement (δ_c) expressed as the following equation, which represents the energy efficiency of the displacement of actuator.[27]

$$\delta_c(t) = \frac{\delta(t)}{Q_d}$$

The value was obtained by dividing the tip displacement (δ) for the initial 5 s by the charge density (Q_d) consumed during that time under an applied voltage of 3 V dc, and the resulting values are summarized in Table 2. The charge density consumed during the actuation of IPMC was calculated by integrating the curve between 0 and 5 s in Figure 5. Indicated
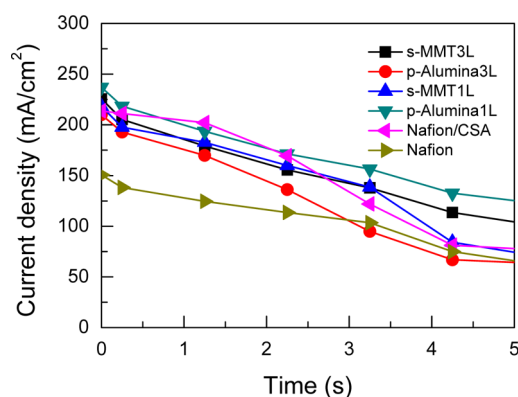

Figure 5. Response current of IPMC actuators based on triple-layered composite membranes for initial 5 s under actuation at 3 V dc.

by these data, the charge-specific displacement greatly increased with the incorporation of the middle layer (Nafion/CSA) into the s-MMT1L- and p-Alumina1L-IPMCs up to the levels of the Nafion- and Nafion/CSA-IPMCs. The higher values of s-MMT3L- and p-Alumina3L-IPMCs were attributed to their much higher displacements per consumed charge for the initial 5 s compared to those of s-MMT1L- and p-Alumina1L-IPMCs. From electromechanical analyses performed in this study, it could be concluded that the fast and large bending actuation of the two triple-layered IPMCs are originated from the effective transport of mobile ions and water, the mechanical gain through the introduction of the higher ion-conductive and less stiff middle layer, and the large accumulation (capacitance) and retention (hygroscopic nature of metal oxides and/or high aspect ratio of MMT) of the mobile species in the outer layers of the two types. Especially, among all samples prepared in the present study, the p-Alumina3L-IPMC displayed the best performance in terms of bending displacement, response rate, back-relaxation, and the energy efficiency of actuation.

CONCLUSIONS

Two designs for triple-layered IPMCs, the s-MMT3L-IPMC and the p-Alumina3L-IPMC, were successfully fabricated via a consecutive solution recasting technique. Compared with the single-layered base samples (Nafion-IPMC and Nafion/CSA-IPMC), both the triple-layered IPMCs exhibited much higher actuation performances in terms of bending displacement, response speed, blocking force, and back-relaxation. The performance improvement was attributed to higher capacitances and Young's moduli, a more efficient transport of mobile ions and water through a faster ionic transport in the middle layer (Nafion/CSA), and a larger accumulation/retention of the mobile species in the outer layers of the two types. Compared with the single-layered counterparts (s-MMT1L-IPMC and p-Alumina1L-IPMC), the bending rates and energy efficiencies of the two triple-layered IPMCs were significantly higher, although the blocking forces were a bit lower. This was considered to be due to a trade-off between displacement and force in terms of the mechanical modulus of the strip. Especially, the p-Alumina3L-IPMC displayed the best actuation performance among all the samples, and the low-voltage-operable character was also observed in the triple-layered IPMC. The present work opens up a new pathway for developing various membrane−electrode−assembly (MEA) structures including IPMCs, fuel cells, batteries, and capacitors with tunable performances by manipulating the functionality of unit layer.

ASSOCIATED CONTENT

Ⓢ Supporting Information

Chemical structure of 10-camphorsulfonic acid (CSA), synthetic procedures for sulfonated montmorillonite (s-MMT) and polypyrrole-coated alumina (p-alumina), a schematic representation showing consecutive solution recasting procedure, X-ray diffraction (XRD) patterns of s-MMT and its Nafion nanocomposites, and a cross-sectional scanning electron microscopy (SEM) image of a Nafion/p-alumina (7.95 wt.%) nanocomposite. This material is available free of charge via the Internet at http://pubs.acs.org.

AUTHOR INFORMATION

Corresponding Author

*E-mail: ytyoo@konkuk.ac.kr. Fax: +82 2 444 0711. Tel.: +82 2 450 3207.

Present Address

§Center for Materials Architecturing, Institute for Multi-Disciplinary Convergence of Materials, Korea Institute of Science and Technology (KIST), Hwarangno 14-gil 5, Seongbuk-gu, Seoul 136-791, Republic of Korea

Notes

The authors declare no competing financial interest.

ACKNOWLEDGMENTS

REFERENCES

(1) Shahinpoor, M.; Bar-Cohen, Y.; Simpson, J. O.; Smith, J. *Smart Mater. Struct.* **1998**, *7*, R15−R30.

(2) Shahinpoor, M.; Kim, K. J. *Smart Mater. Struct.* **2001**, *10*, 819−833.

(3) Lu, J.; Kim, S.-G.; Lee, S.; Oh, I.-K. *Adv. Funct. Mater.* **2008**, *18*, 1290−1298.

(4) Lee, J. Y.; Wang, H. S.; Yoon, B. R.; Han, M. J.; Jho, J. Y. *Macromol. Rapid Commun.* **2010**, *31*, 1897−1902.

(5) Lee, J.-W.; Hong, S. M.; Kim, J.; Koo, C. M. *Sens. Actuators, B* **2012**, *162*, 369−376.

(6) Lee, J.-W.; Yu, S.; Hong, S. M.; Koo, C. M. *J. Mater. Chem. C* **2013**, *1*, 3784−3793.

(7) Cha, Y.; Shen, L.; Porfiri, M. *Smart Mater. Struct.* **2013**, *22*, 055027.

(8) Akle, B. J.; Leo, D. J.; Hickner, M. A.; McGrath, J. E. *J. Mater. Sci.* **2005**, *40*, 3715−3724.

(9) Phillips, A. K.; Moore, R. B. *Polymer* **2005**, *46*, 7788−7802.

(10) Lee, J.-W.; Kim, J.-H.; Goo, N. S.; Lee, J. Y.; Yoo, Y.-T. *J. Bionic Eng.* **2010**, *7*, 19−28.

(11) Luqman, M.; Lee, J.-W.; Moon, K.-K.; Yoo, Y.-T. *J. Ind. Eng. Chem.* **2011**, *17*, 49−55.

(12) Chao, W.-K.; Lee, C.-M.; Tsai, D.-C.; Chou, C.-C.; Hsueh, K.-L.; Shieu, F.-S. *J. Power Sources* **2008**, *185*, 136−142.

(13) Huang, Q. M.; Zhang, Q. L.; Huang, H. L.; Li, W. S.; Huang, Y. J.; Luo, J. L. *J. Power Sources* **2008**, *184*, 338−343.

(14) Nam, J. D.; Choi, H. R.; Tak, Y. S.; Kim, K. J. *Sens. Actuators, A* **2003**, *105*, 83−90.

(15) Lee, D. Y.; Park, I.-S.; Lee, M.-H.; Kim, K. J.; Heo, S. *Sens. Actuators, A* **2007**, *133*, 117−127.

(16) Palmre, V.; Brandell, D.; Mäeorg, U.; Torop, J.; Volobujeva, O.; Punning, A.; Johanson, U.; Kruusmaa, M.; Aabloo, A. *Smart Mater. Struct.* **2009**, *18*, 095028.

(17) Akle, B. J.; Bennett, M. D.; Leo, D. J. *Sens. Actuators, A* **2006**, *126*, 173−181.

(18) Lee, J.-W.; Lee, J. H.; Kim, M.; Hong, S. M.; Koo, C. M. *J. Nanosci. Nanotechnol.* **2013**, *13*, 3606−3610.

(19) Lee, J.-W.; Kim, J.-H.; Chun, Y. S.; Yoo, Y. T.; Hong, S. M. *Macromol. Res.* **2009**, *17*, 1032−1038.

(20) Fukushima, T.; Asaka, K.; Kosaka, A.; Aida, T. *Angew. Chem. Int. Ed.* **2005**, *44*, 2410−2413.

(21) Moore, R. B.; Martin, C. R. *Anal. Chem.* **1986**, *58*, 2569−2570.

(22) Moore, R. B.; Martin, C. R. *Macromolecules* **1988**, *21*, 1334−1339.

(23) Fu, T.; Cui, Z.; Zhong, S.; Shi, Y.; Zhao, C.; Zhang, G.; Shao, K.; Na, H.; Xing, W. *J. Power Sources* **2008**, *185*, 32−39.

(24) Nguyen, V. K.; Lee, J. W.; Yoo, Y. *Sens. Actuators, B* **2007**, *120*, 529−537.

(25) Han, M. J.; Park, J. H.; Lee, J. Y.; Jho, J. Y. *Macromol. Rapid Commun.* **2006**, *27*, 219−222.

(26) Yeh, C.-C.; Shih, W.-P. *Smart Mater. Struct.* **2010**, *19*, 124007.

(27) Lee, J.-W.; Yoo, Y.-T. *Sens. Actuators, B* **2009**, *137*, 539−546.